Romanian Reports in Physics **72**, 508 (2020)

FEW-CYCLE ACOUSTIC SOLITONS IN A STRAINED PARAMAGNET

S. V. SAZONOV[1,2,*], N. V. USTINOV[3,4]

[1]National Research Centre "Kurchatov Institute", Moscow 123182, Russia
[2]Moscow Aviation Institute (National Research University), Moscow 125993, Russia
[*]Email: *sazonov.sergey@gmail.com*
[3]Kaliningrad Institute of Management, Kaliningrad 236001, Russia
[4]Lomonosov Moscow State University, Moscow 119991, Russia

Received July 7, 2020

Abstract. The theoretical investigation of propagation of few-cycle transverse acoustic solitons in a cubic paramagnetic crystal placed in an external magnetic field and in a field of static deformation is carried out. The self-consistent system of nonlinear equations for the spin variables and relative deformation of the acoustic pulse is derived. This system generalizes the system of the reduced Maxwell–Bloch equations, well-known in nonlinear optics, and occurs to be also integrable by the inverse scattering transformation method. The soliton and breather solutions of the obtained system are investigated in detail. It is revealed that the properties of the solitons and breathers depend on the ratio between the frequencies of the Zeeman and quadrupole Stark splittings of the effective spins of the paramagnet. If the Zeeman splitting exceeds the Stark one, then the short-living pulse of the deformation field, whose dynamics is similar to that of rogue waves, can be formed under the collision of two solitons having different polarities. In the opposite case, the soliton collision does not lead to the appearance of such pulse of the deformation field. Here, the duration of the soliton is limited from below by the minimal value at which the profile of relative deformation has a rectangular shape.

Key words: few-cycle acoustic pulse, soliton, acoustic self-induced transparency, generalized reduced Maxwell–Bloch equations.

1. INTRODUCTION

The effect of the self-induced transparency (SIT) [1, 2] is the first experimental observation of a soliton in nonlinear optics. This stimulated, in turn, subsequent intensive theoretical and experimental studies of the SIT [3, 4].

The SIT soliton propagates without losses in the absorbing medium and causes its strong excitation. This decreases significantly the soliton velocity: it can be less than the speed of light in vacuum by two or even four orders of magnitude.

The laser pulses with nano- and picosecond durations contain from millions to thousands light oscillations. As a result, their spectrum is rather narrow and is concentrated near the carrier frequency ω, *i. e.* these pulses are quasimonochromatic. The approximation of the slowly varying envelopes (SVE) is usually applied under the theoretical investigations of nonlinear interaction of such pulses with matter [5].

The quasimonochromaticity of the light pulses gives an opportunity to simplify considerably the quantum model of the medium through which they propagate. It is possible in the case of the resonant interaction of the pulses with a matter to use the model of the two-level atoms to describe its dynamics. This implies an allocation of the two quantum levels that have the transition frequency ω_0 close to the carrier frequency of the light pulses.

Since the SIT is a resonant effect, the SVE approximation and the model of the two-level atoms proved very good for theoretical researches of this phenomenon. The SVE approximation allowed simplifying considerably the initial nonlinear system of the wave and material equations. Neglecting the second-order derivatives of the envelopes of the electric field succeeded to reduce the wave equation to the derivatives of the first order. The material equations underwent also considerable simplifications due to the SVE approximation.

This way, the system of the so-called SIT equations was derived [6–8]. This system occurred to be integrable in the framework of the inverse scattering transformation (IST) method [6, 7, 9, 10] and has multisoliton solutions. At zero detuning of the carrier frequency of pulses from the frequency of allocated quantum transition (the case of exact resonance), the SIT equations are reduced to the sine-Gordon (SG) equation for the integral of the pulse electric field on the temporal variable [3, 6].

An alternative approach to describe the SIT effect, in which the SVE approximation is not used, was offered in Ref. [11]. At the same time, the model of two-level atoms was exploited. It was supposed, however, that the concentration of the atoms is small enough. This allowed to apply the unidirectional propagation (UP) approximation and to reduce the initial wave equation to that of the first order. It is important to note that this equation and the material ones contain the electric field of the pulse rather than its envelopes. The equations obtained in such manner were called the system of the reduced Maxwell–Bloch (RMB) equations. This system is also integrable by the IST method, and its multisoliton and breather solutions were found [7, 11].

The breathers of the RMB system may contain any number of the oscillations. It can be shown that the breathers with a large number of oscillations pass into the solitons of the envelope of the SIT system. The propagation velocity of such breathers differs insignificantly from the speed of light in vacuum because of the small concentration of the atoms.

The breathers containing a small number of oscillations correspond to the so-called few-cycle pulses (FCPs). These pulses are broadband. So, the spectral width of the single-cycle pulse has an order of its central frequency. As a result, the concept of the carrier frequency loses its meaning [12–20].

The spectrum of the FCP may capture not only one quantum transition. Several transitions can be involved simultaneously into the interaction with such pulse. For this reason, the question of the applicability of the model of two-level atoms rises.

The model of the medium consisting of two sorts of two-level atoms with strongly differing frequencies of the quantum transitions was applied to describe the interaction of the FCP with matter in Refs. [16, 17, 20].

The two-level model was modified in Refs. [21–23]. by an addition to the pair of allocated quantum levels of the ones lying above on the energy scale. As a result, the generalized SG (GSG) equation [21, 22] and the generalized RMB (GRMB) system [23], which is reduced in the particular cases to the GSG equation, were obtained. The GSG equation and the GRMB system were found to be integrable by means of the IST method [22–24]. New solitonic (unipolar) and breather solutions and the modes of their interaction with each other were studied in details.

It developed usually that the nonlinear optical phenomena found their acoustic counterparts after a short time [25, 26]. The SIT effect does not become an exception here. So, the effect of the acoustic SIT (ASIT) on the system of resonant paramagnetic impurities of the crystal placed in an external magnetic field was investigated [27–30]. The experimental studies of the ASIT were carried out in Refs. [27, 30] in the case of the longitudinal acoustic pulses of hypersonic frequencies ($\omega \sim 10^{11}$ s^{-1}). The transverse acoustic pulses were considered in Ref. [29].

Next, various theoretical generalizations of the ASIT effect were suggested. So, the ASIT for the longitudinal-transverse waves was investigated [31–37]. The theoretical research of the ASIT in the conditions of the acoustic Stark effect was carried out also [38–40]. In this case, the ASIT effect is followed by the acoustic rectification and the generation of high harmonics. The ASIT of the three-component (longitudinal-transverse) acoustic pulses was considered in [40].

A development of the approach relied on the analogy between optical and acoustic phenomena can be carried out by searching the conditions, under which a realization of acoustic variant of the GRMB system is possible. An investigation of various soliton and breather solutions can reveal here the distinctive features inherent only in the acoustic localized structures. The present paper is dedicated to studying such development.

The paper is organized as follows. In Sec. 2, the system of self-consistent equations describing the interaction of the transverse acoustic pulse with paramagnetic ions possessing the effective spin $S = 1$ is derived. Also, this system is approximately reduced here to the acoustic variant of the GRMB system. In Sec. 3, the soliton and breather solutions are considered, and the interaction between them is investigated. In the Conclusion, the main results are summarized and some prospects of further studies are outlined.

2. GENERALIZED REDUCED SYSTEM OF THE MAXWELL–BLOCH TYPE

The strongest interaction with the vibrations of the lattice sites is experienced by the paramagnetic ions possessing the effective spin $S = 1$ [41]. This is the case, for example, of the paramagnetic ions Fe^{2+} introduced in the cubic crystal MgO [27].

The interaction of the acoustic field with the paramagnetic ions (spin-phonon coupling) is realized through the Van Vleck mechanism [41] that consists in the following. The elastic field causes the local deformation of the crystal lattice. This produces the gradients of the intracrystalline electric field that, in turn, induce the quadrupole transitions between Zeeman sublevels and the shift of the frequencies of these transitions because of the quadrupole Stark effect.

Let the cubic crystal be placed in the external magnetic field $\mathbf{B}$ parallel to the z axis and is subjected to the longitudinal static deformation ε_0 along this axis. We assume here that the x, y, and z axes of the Cartesian coordinate system coincide with the fourth-order symmetry axes of the crystal.

Suppose that the wave of the shift deformation propagates in the crystal along the x axis. This wave is characterized by the component of the deformation tensor $\varepsilon \equiv \varepsilon_{zx} = \frac{1}{2}\frac{\partial u_z}{\partial x}$, where u_z is the local displacement of the crystal sites in the direction of the z axis.

Under the conditions specified above, the Hamiltonian operator for the paramagnetic ion is written as follows [41, 42]:

$$\hat{H}_S = \hat{H}_0 + \hat{H}_{int}, \tag{1}$$

where

$$\hat{H}_0 = \hbar\omega_Z \hat{S}_z + \hbar\omega_S \hat{S}_z^2, \tag{2}$$

$$\hat{H}_{int} = \frac{1}{2} G_\perp \left(\hat{S}_x \hat{S}_z + \hat{S}_z \hat{S}_x \right) \frac{\partial u_z}{\partial x}, \tag{3}$$

the frequencies of the Zeeman and quadrupole Stark splittings are defined as given

$$\omega_Z = \frac{g\mu_B B}{\hbar}, \quad \omega_S = \frac{G_\parallel \varepsilon_0}{\hbar}, \tag{4}$$

$\hbar$ is the Planck constant, g is the Landé factor, μ_B is the Bohr magneton, $G_\parallel$ and $G_\perp$ are the components of the tensor of the spin-phonon coupling, and $\hat{S}_z$ and $\hat{S}_z$ are the spin matrices

$$\hat{S}_z = \begin{pmatrix} -1 & 0 & 0 \\ 0 & 0 & 0 \\ 0 & 0 & 1 \end{pmatrix}, \quad \hat{S}_x = \frac{1}{\sqrt{2}} \begin{pmatrix} 0 & 1 & 0 \\ 1 & 0 & 1 \\ 0 & 1 & 0 \end{pmatrix}. \tag{5}$$

We exploit below the semiclassical approach, in which the strain field is considered in the classical manner, while the paramagnetic ion is described as a quantum object.

According to this approach, we write the classical Hamiltonian for the field of shift deformation

$$H_e = \frac{1}{2}\int \left\{ \frac{p_z^2}{\rho} + \rho a_\perp^2 \left(\frac{\partial u_z}{\partial x} \right) \right\} \mathrm{d}^3\mathbf{r}, \tag{6}$$

where ρ is the the equilibrium crystal density, $a_\perp$ is the linear velocity of the transverse sound, p_z is the momentum density of local displacements in the crystal. The integration is performed over the entire crystal volume.

The dynamics of the quantum states of the paramagnetic ion is governed by the von Neumann equation

$$\mathrm{i}\hbar \frac{\partial \hat{\rho}}{\partial t} = [\hat{H}_S, \hat{\rho}], \tag{7}$$

where the density matrix $\hat{\rho}$ of the effective spin $S = 1$ is represented as

$$\hat{\rho} = \begin{pmatrix} \rho_{33} & \rho_{32} & \rho_{31} \\ \rho_{23} & \rho_{22} & \rho_{21} \\ \rho_{13} & \rho_{12} & \rho_{11} \end{pmatrix}. \tag{8}$$

The field of deformations is described by the canonical equations of the mechanics of the continuous media

$$\frac{\partial p_z}{\partial t} = -\frac{\delta H}{\delta u_z}, \quad \frac{\partial u_z}{\partial t} = \frac{\delta H}{\delta p_z}, \tag{9}$$

where

$$H = H_e + \langle \hat{H}_{int} \rangle, \tag{10}$$

the quantum average of the Hamiltonian of spin-phonon coupling is defined in the following manner:

$$\langle \hat{H}_{int} \rangle = n \int \mathrm{Tr}\left(\hat{\rho} \hat{H}_{int} \right) \mathrm{d}^3\mathbf{r}, \tag{11}$$

where n is the concentration of the paramagnetic ions.

From Eqs. (7), (8), and (1)–(3), we obtain the system of the material equations for the elements of the density matrix

$$\frac{\partial \rho_{21}}{\partial t} = -\mathrm{i}\omega_0 \rho_{21} - \mathrm{i}\Omega(\rho_{22} - \rho_{11} + \rho_{31}), \tag{12}$$

$$\frac{\partial \rho_{22}}{\partial t} = -\mathrm{i}\Omega(\rho_{32} - \rho_{32}^* + \rho_{21} - \rho_{21}^*), \tag{13}$$

$$\frac{\partial \rho_{11}}{\partial t} = \mathrm{i}\Omega(\rho_{21} - \rho_{21}^*), \tag{14}$$

$$\frac{\partial \rho_{33}}{\partial t} = \mathrm{i}\Omega(\rho_{32} - \rho_{32}^*), \tag{15}$$

$$\frac{\partial \rho_{31}}{\partial t} = -\mathrm{i}\omega_{31}\rho_{31} - \mathrm{i}\Omega(\rho_{21} + \rho_{32}), \tag{16}$$

$$\frac{\partial \rho_{32}}{\partial t} = -\mathrm{i}\omega_{32}\rho_{32} + \mathrm{i}\Omega(\rho_{33} - \rho_{22} - \rho_{31}), \tag{17}$$

where (see Fig. 1a and 1b)

$$\begin{aligned} &\omega_0 \equiv \omega_{21} = |\omega_Z - \omega_S|, \quad \omega_{32} = \min\{\omega_Z + \omega_S, 2\omega_Z\}, \\ &\omega_{31} = \max\{\omega_Z + \omega_S, 2\omega_Z\}, \end{aligned} \tag{18}$$

$$\Omega = \frac{G_\perp}{2\sqrt{2}\hbar}\frac{\partial u_z}{\partial x} = \frac{G_\perp \varepsilon}{\sqrt{2}\hbar}. \tag{19}$$

Combining Eqs. (9)–(11), (8), (3), (5) and (19), we derive the wave equation

$$\frac{\partial^2 \Omega}{\partial x^2} - \frac{1}{a_\perp^2}\frac{\partial^2 \Omega}{\partial t^2} = \frac{nG_\perp^2}{8\hbar\rho a_\perp^2}\frac{\partial^2}{\partial x^2}\left(\rho_{21} + \rho_{21}^* - \rho_{32} - \rho_{32}^*\right). \tag{20}$$

Thus, we have the self-consistent system of the equations (12)–(17) and (20).

The magnetic field removes the degeneration on the projection of the effective spin S_z. In turn, the static deformation ε_0 removes the degeneration on the modulus of S_z. The splitting of the spin sublevels is presented in Fig. 1a and 1b for the cases $\omega_Z > \omega_S$ and $\omega_Z < \omega_S$, respectively. It is seen that one case passes into another under the replacement $1 \leftrightarrow 2$. In this regard, we firstly consider the case $\omega_Z > \omega_S$.

Assume that $|\omega_Z - \omega_S| \ll \omega_Z,\ \omega_S$. In the designations accepted in Eqs. (12)–(17), this corresponds to inequalities

$$\omega_0 \ll \omega_{31},\ \omega_{32}. \tag{21}$$

Let τ_* be the characteristic time scale of the elastic pulse. Suppose that the condition of the transparency for transitions $2 \leftrightarrow 3$ and $1 \leftrightarrow 3$ is fulfilled:

$$\mu \sim (\omega_{31}\tau_*)^{-1} \sim (\omega_{32}\tau_*)^{-1} \ll 1. \tag{22}$$

The formal restrictions on transition $1 \leftrightarrow 2$ are not imposed.

We assume also that the populations of the two first quantum levels before the impact of the elastic pulse on the crystal are equal to w_1 and w_2, respectively. At the same time, the third (remote) level is not populated.

Let us exclude from Eqs. (12)–(17) the density matrix elements corresponding to the transitions $2 \leftrightarrow 3$ and $1 \leftrightarrow 3$. We restrict ourselves by the first-order approximation with respect to the small parameter μ. In accordance with this, equalizing the

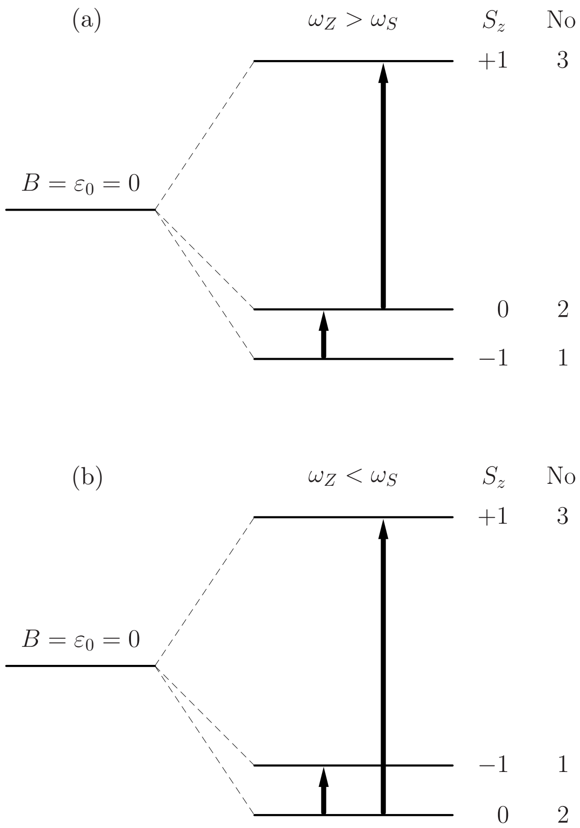

Fig. 1 – The spin sublevels and the allowed spin-phonon transitions for $\omega_Z > \omega_S$ (a) and $\omega_Z < \omega_S$ (b).

left-hand sides of Eqs. (16) and (17) to zero, we obtain

$$\rho_{31} = -\Omega\,\frac{\rho_{21}+\rho_{32}}{\omega_{31}} \approx -\Omega\,\frac{\rho_{21}}{\omega_{31}}, \tag{23}$$

$$\rho_{32} = \Omega\,\frac{\rho_{33}-\rho_{22}}{\omega_{32}} - \Omega\,\frac{\rho_{31}}{\omega_{32}} \approx \Omega\,\frac{\rho_{33}-\rho_{22}}{\omega_{32}}. \tag{24}$$

The substitution of expression (23) into (12) yields

$$\frac{\partial\rho_{21}}{\partial t} = -\mathrm{i}\left(\omega_0 - \frac{\Omega^2}{\omega_{31}}\right)\rho_{21} - \mathrm{i}\Omega(\rho_{22}-\rho_{11}). \tag{25}$$

We have $\frac{\partial\rho_{33}}{\partial t} = 0$ from Eqs. (15) and (24). Thus, it is necessary in the first order on the small parameter μ to neglect the population of the third quantum level: $\rho_{33} = 0$. Then, we find from Eq. (24)

$$\rho_{32} = -\Omega\,\frac{\rho_{22}}{\omega_{32}}. \tag{26}$$

By substituting now expression (26) into Eq. (13), we obtain

$$\frac{\partial \rho_{22}}{\partial t} = -\mathrm{i}\Omega(\rho_{21} - \rho_{21}^*). \tag{27}$$

The system (25), (14), and (27) can be rewritten in the terms of the Bloch variables

$$U = \frac{\rho_{21} + \rho_{21}^*}{2}, \quad V = \frac{\rho_{21}^* - \rho_{21}}{2\mathrm{i}}, \quad W = \frac{\rho_{22} - \rho_{11}}{2}. \tag{28}$$

Then

$$\frac{\partial U}{\partial t} = -(\omega_0 - \beta\Omega^2)V, \tag{29}$$

$$\frac{\partial V}{\partial t} = (\omega_0 - \beta\Omega^2)U + 2\Omega W, \tag{30}$$

$$\frac{\partial W}{\partial t} = -2\Omega V, \tag{31}$$

where

$$\beta = \frac{1}{\omega_{31}}. \tag{32}$$

Taking into account relations (26) and (28), we represent the expression in the brackets in the right-hand side of Eq. (20) in the following manner:

$$\rho_{21} + \rho_{21}^* - \rho_{32} - \rho_{32}^* = 2\left(U + \Omega\,\frac{\rho_{22}}{\omega_{32}}\right).$$

Since $\rho_{22} + \rho_{11} = 1$ within the approximations accepted, we find from the last relation in Eqs. (28) that $\rho_{22} = \frac{1}{2} + W$. Therefore,

$$\rho_{21} + \rho_{21}^* - \rho_{32} - \rho_{32}^* = \frac{\Omega}{\omega_{32}} + 2\left(U + \Omega\,\frac{W}{\omega_{32}}\right).$$

According to inequality (21), we write $\omega_{32} \approx \omega_{31}$. Then, taking into account expression (32), we put

$$\rho_{21} + \rho_{21}^* - \rho_{32} - \rho_{32}^* = \frac{\Omega}{\omega_{31}} + 2\,(U + \beta\Omega W) \tag{33}$$

with a good accuracy.

In the case considered, the inequality

$$\frac{nG_\perp^2}{8\hbar\omega_{31}\rho a_\perp^2} \ll 1 \tag{34}$$

is satisfied well. Then, the second-order equation (20) is reduced to that of the first order

$$\frac{\partial \Omega}{\partial x} + \frac{1}{a_\perp}\frac{\partial \Omega}{\partial t} = -\frac{nG_\perp^2}{4\hbar\rho a_\perp^3}\frac{\partial}{\partial t}(\rho_{21} + \rho_{21}^* - \rho_{32} - \rho_{32}^*).$$

Substituting expression (33) here and taking into account (34), we finally obtain

$$\frac{\partial \Omega}{\partial x}+\frac{1}{a_\perp}\frac{\partial \Omega}{\partial t}=-\alpha\frac{\partial}{\partial t}(U+\beta\Omega W), \tag{35}$$

where

$$\alpha=\frac{nG_\perp^2}{8\hbar\rho a_\perp^2}.$$

Such procedure implies that the backscattering from the paramagnetic impurities is neglected [11].

Thus, the system (29)–(31), (35) describes in the case $\omega_Z > \omega_S$ the interaction of the elastic pulses with the paramagnetic impurities.

The consideration in the case $\omega_Z < \omega_S$ gives also the system (29)–(31), (35), where parameter β is defined now in the following manner:

$$\beta=-\frac{1}{\omega_{31}}. \tag{36}$$

As a result, the system (29)–(31), (35) is valid in both cases. We have $\beta > 0$, if $\omega_Z > \omega_S$ (Fig. 1a), and $\beta < 0$, if $\omega_Z < \omega_S$ (Fig. 1b). Taking into account Eqs. (18), we see that the general expression for parameter β has the following form:

$$\beta=\frac{\mathrm{sgn}\,(\omega_Z-\omega_S)}{2\omega_Z}. \tag{37}$$

It was supposed under the derivation of the system (29)–(31), (35) that the third (upper) quantum level remains unpopulated. Let us assume that the paramagnetic ions are in the thermodynamic equilibrium state before the impact of the elastic pulse. Then, it is possible to neglect the population of the third level if $\hbar\omega_Z/k_BT \gg 1$, where k_B is the Boltzmann constant and T is the absolute temperature. In the experiments on the paramagnetic resonance, the Zeeman splittings with frequencies $\omega_Z \sim 10^{12}$ s^{-1} are reached. Then, we have $\hbar\omega_Z/k_BT \sim 10$ at $T \sim 1$ K.

The condition $\omega_0 \ll \omega_Z$ imposed under the derivation of the system (29)–(31), (35) is equivalent to inequality $|\omega_Z-\omega_S|/\omega_Z \ll 1$. This gives $\omega_Z \approx \omega_S$. From this and relations (4), it follows that $\varepsilon_0 \sim \hbar\omega_Z/G_\parallel$. Taking $G_\parallel \sim 10^{-13}$ Erg, we find $\varepsilon_0 \sim 10^{-2}$. At the same time, $\omega_0 \sim 10^{11}$ s^{-1}.

Thus, the conditions accepted under the derivation of the self-consistent system (29)–(31), (35) can be realized in an experiment.

3. ACOUSTIC SOLITONS AND BREATHERS

The system (29)–(31), (35) is the acoustic variant of the GRMB system [23, 24] and is connected by means of the change of variables with the system of the modified

RMB (MRMB) equations

$$\frac{\partial U_0}{\partial T} = -2\omega_0\sqrt{1-\varepsilon^2\Omega_0^2}\,V_0, \tag{38}$$

$$\frac{\partial V_0}{\partial T} = 2\omega_0\sqrt{1-\varepsilon^2\Omega_0^2}\,U_0 + \Omega_0 W_0, \tag{39}$$

$$\frac{\partial W_0}{\partial T} = -\Omega_0 V_0, \tag{40}$$

$$\frac{\partial \Omega_0}{\partial X} = -\frac{1}{\omega_0}\frac{\partial U_0}{\partial T}. \tag{41}$$

This system coincides with the RMB equations [11] in the case $\varepsilon = 0$ and is also integrable by the IST method.

The change of variables $(T, X, \Omega_0, U_0, V_0, W_0) \to (t, x, \Omega, U, V, W)$ reducing the MRMB equations (38)–(41) to the system (29)–(31), (35) is defined by the following relations:

$$\begin{aligned}
&\mathrm{d}t = \left[1+\sqrt{1-\varepsilon^2\Omega_0^2}\right]\mathrm{d}T + \left[2\varepsilon^2 W_0 + \frac{1}{\omega_0\alpha a_\perp}\right]\mathrm{d}X, \quad \mathrm{d}x = \frac{\mathrm{d}X}{\omega_0\alpha},\\
&\Omega(t,x) = \frac{1}{2}\frac{\Omega_0(T,X)}{1+\sqrt{1-\varepsilon^2\Omega_0^2(T,X)}}, \quad W(t,x) = W_0(T,X),\\
&U(t,x) = V_0(T,X), \quad V(t,z) = -U_0(T,X),
\end{aligned} \tag{42}$$

where

$$\varepsilon = \sqrt{\frac{\beta}{4\omega_0}}. \tag{43}$$

The change of variables (42) allows us to construct the multisoliton solutions of the system (29)–(31), (35) from ones of the MRMB equations (38)–(41). In Refs. [24, 39], the multisoliton solutions of the MRMB equations were obtained by means of the Darboux transformation technique [43–45] and were studied in details. It is assumed below that the asymptotic values of variables U_0, V_0, and W_0 are equal to 0, 0, and $W_0^{(0)} = (w_2 - w_1)/2$, respectively.

3.1. THE CASE $\omega_Z > \omega_S$.

The variable Ω_0 of the one-soliton solution of the MRMB equations (38)–(41) is written as follows:

$$\Omega_0 = \pm 2\sqrt{A}\,\frac{\cosh\theta}{A\cosh^2\theta + \varepsilon^2}, \tag{44}$$

where

$$A = \frac{1}{4\nu^2} - \varepsilon^2\left(1 + \frac{\omega_0^2}{\nu^2}\right), \quad \theta = 2\nu\left(T - \frac{W_0^{(0)} X}{\nu^2 + \omega_0^2}\right) + \theta_0,$$

ν and θ_0 are real constants. Without loss of generality, we will put $\theta_0 = 0$. It is assumed in these formulas that $|\nu| < |\sigma/\varepsilon|$, where

$$\sigma = \frac{\sqrt{1-\beta\omega_0}}{2}. \tag{45}$$

From Eq. (44), we find

$$\max|\Omega_0| = \begin{cases} \dfrac{2|\nu|}{|\sigma|}\sqrt{1-\nu^2\dfrac{\varepsilon^2}{\sigma^2}} & \text{for } |\nu| < \dfrac{|\sigma|}{\sqrt{2}|\varepsilon|}, \\ \dfrac{1}{|\varepsilon|} & \text{for } \dfrac{|\sigma|}{\sqrt{2}|\varepsilon|} \le |\nu| < \dfrac{|\sigma|}{|\varepsilon|}. \end{cases} \tag{46}$$

The profile of Ω_0 consists of two peaks in the second case ($|\sigma/\sqrt{2}\varepsilon| \le |\nu| < |\sigma/\varepsilon|$). These peaks have the same polarities. The interval between them is determined by the value of the parameter ν. In the first case ($|\nu| < |\sigma/\sqrt{2}\varepsilon|$), the profile of Ω_0 consists of one peak.

The variable Ω of the one-soliton solution of the system (29)–(31), (35) is defined implicitly by the substitution of the expression (44) into Eqs. (42). The first relation in (42) gives

$$t = 2T + \frac{\varepsilon}{2\sigma}\ln\left[\frac{\sigma-\nu\varepsilon\tanh\theta}{\sigma+\nu\varepsilon\tanh\theta}\right] + \left(2\varepsilon^2 W_0 + \frac{1}{\omega_0\alpha a_\perp}\right)X.$$

This relation implies that the one-soliton solution of the system (29)–(31), (35) is steady-state. It follows from Eqs. (42)–(45) that

$$\max|\Omega| = \frac{1}{2}\frac{|\nu|}{\sqrt{\sigma^2-\nu^2\varepsilon^2}}. \tag{47}$$

If $|\nu| \to |\sigma/\varepsilon|$, then the amplitude of the variable Ω tends to infinity.

The profiles of the variable Ω of the one-soliton solutions of the system (29)–(31), (35) for different values of parameter ν are presented in Fig. 2.

It is seen that the amplitude of the soliton is not proportional to its inverse duration as opposite to the case of the RMB system.

Note that the change of variables (42) transforms the soliton of the MRMB equations with two peaks ($|\sigma/\sqrt{2}\varepsilon| \le |\nu| < |\sigma/\varepsilon|$) into the soliton of the system (29)–(31), (35) with a single peak. This is a result of the change of the sign by the square root in Eqs. (42) between the peaks of variable Ω_0.

The expression for variable Ω_0 of the two-soliton solution of the MRMB equa-

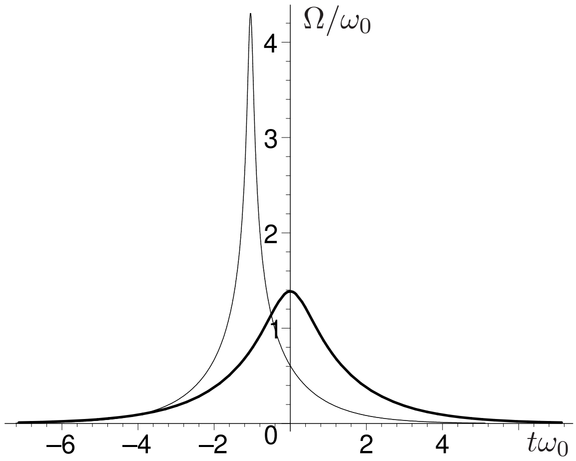

Fig. 2 – Profiles of the variable Ω of one-soliton solution with parameters $\beta = 1/32\omega_0$, $W_0^{(0)} = -1/2$, $X = 0$, and $\nu = 0.95\omega_0$ (normal line), $\nu = 0.7\omega_0$ (bold line).

tions (38)–(41) has the form:

$$\begin{aligned}\Omega_0 = \ & \frac{1}{\sigma}\frac{\partial}{\partial T}\left(\arctan\frac{\nu_+ \sinh\theta_-}{\nu_- \cosh\theta_+}\right. \\ & \left. + \arctan\frac{\nu_+[\eta_- \sinh\theta_- - 2\nu_-\varepsilon\sigma\cosh\theta_-]}{\nu_-[\eta_+ \cosh\theta_+ - 2\nu_+\varepsilon\sigma\sinh\theta_+]}\right),\end{aligned} \tag{48}$$

Here

$$\nu_\pm = \frac{\nu_1 \pm \nu_2}{2}, \quad \theta_\pm = \frac{\theta_1 \pm \theta_2}{2}, \quad \eta_\pm = \sigma^2 \pm \nu_1\nu_2\varepsilon^2,$$

$$\theta_{1,2} = 2\nu_{1,2}\left(T - \frac{W_0^{(0)} X}{\nu_{1,2}^2 + \omega_0^2}\right) + \theta_{1,2}^{(0)} + ik_{1,2}\pi,$$

$\nu_{1,2}$, $\theta_{1,2}^{(0)}$ are the real constants, $|\nu_{1,2}| < |\sigma/\varepsilon|$, and the parameters k_1 and k_2 take values 0 or 1. The shifts of the independent variables allow us to put $\theta_1^{(0)} = \theta_2^{(0)} = 0$ without loss of generality.

This solution describes the collision of the solitons of the MRMB equations. The implicit definition of variable Ω of the two-soliton solution of the system (29)–(31), (35) is obtained by the substitution of the expression (48) into Eqs. (42). Consider the collision of the solitons of this system in details.

If $(-1)^{k_1+k_2}\nu_1\nu_2 < 0$, then the two-soliton solution describes the interaction of the solitons of the same polarities. The process of the interaction is similar to that of the solitons in the cases, for example, of the RMB system, the Korteweg–de Vries or modified Korteweg–de Vries equations [46, 47].

If $(-1)^{k_1+k_2}\nu_1\nu_2 > 0$, then the two-soliton solution of the system (29)–(31), (35) describes the interaction of solitons with opposite polarities. We point out that in the case $|\nu_1|,\ |\nu_2| \ll |\sigma/\sqrt{2}\varepsilon|$, the amplitudes of the variable Ω of these solitons are much smaller than $1/|\varepsilon|$ (see Eq. (47)). The interaction of such solitons is similar to that for the modified Korteweg–de Vries or RMB equations and is accompanied by the appearance of a pulse having amplitude equal almost to the sum of the amplitudes of the colliding solitons [46, 47].

The distinguishing feature in the interaction of the solitons takes place in the case when $|\nu_1| \approx |\sigma/\sqrt{2}\varepsilon|$ or/and $|\nu_2| \approx |\sigma/\sqrt{2}\varepsilon|$. Here, the amplitude of the variable Ω of the one of the solitons at least is close to $1/|\varepsilon|$. The collision of such solitons leads to an appearance of the short-living pulse with extraordinarily large amplitude or even to the blow-up of the two-soliton solution.

The main stages of the collision of the solitons of the system (29)–(31), (35) in the case of opposite polarities are presented in Fig. 3.

The amplitude of the short-living pulse of variable Ω appearing under the soliton interaction exceeds significantly the sum of the amplitudes of the colliding solitons (Fig. 3b). The dynamics of such short-living pulse is similar to that of the rogue waves [48–58].

The expression for variable Ω_0 of the breather solution of the MRMB equations (38)–(41) is written in the following manner:

$$\begin{aligned}\Omega_0 = \ & \frac{1}{\sigma}\frac{\partial}{\partial T}\left(\arctan\frac{\nu_R \sin\theta_I}{\nu_I\cosh\theta_R}\right.\\ & \left. + \arctan\frac{\nu_R\left[(\sigma^2 - |\nu|^2\varepsilon^2)\sin\theta_I - 2\nu_I\varepsilon\sigma\cos\theta_I\right]}{\nu_I\left[(\sigma^2 + |\nu|^2\varepsilon^2)\cosh\theta_R - 2\nu_R\varepsilon\sigma\sinh\theta_R\right]}\right),\end{aligned} \tag{49}$$

where

$$\theta_R = 2\nu_R\left[T - \frac{W_0^{(0)}(\nu_R^2+\nu_I^2+\omega_0^2)X}{\nu_R^4 + 2(\nu_I^2+\omega_0^2)\nu_R^2 + (\nu_I^2-\omega_0^2)^2}\right] + \theta_{R,0},$$

$$\theta_I = 2\nu_I\left[T + \frac{W_0^{(0)}(\nu_R^2+\nu_I^2-\omega_0^2)X}{\nu_R^4 + 2(\nu_I^2+\omega_0^2)\nu_R^2 + (\nu_I^2-\omega_0^2)^2}\right] + \theta_{I,0},$$

ν_R, ν_I, $\theta_{R,0}$, and $\theta_{I,0}$ are real constants, $|\nu|^2 = \nu_R^2 + \nu_I^2$. In what follows, we use the shifts of the independent variables to put $\theta_{R,0} = \theta_{I,0} = 0$.

The implicit definition of variable Ω of the breather solution of the system (29)–(31), (35) is obtained by the substitution of expression (49) into Eqs. (42). Figure 4 shows the profiles of variable Ω of this solution for different values of the parameter ν_I determining the breather carrier frequency for the most part.

When the carrier frequency is high enough, the breather solution is similar to that of the RMB equations (see the plot with bold line). If the carrier frequency tends

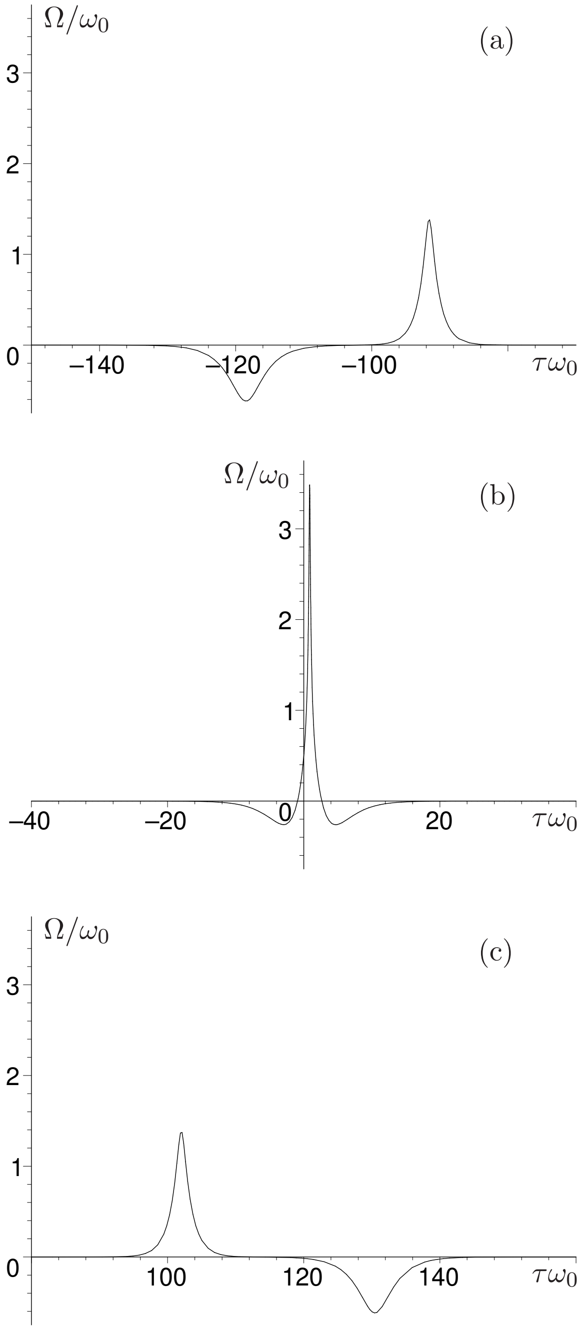

Fig. 3 – Profiles of the variable Ω of two-soliton solution with parameters $\beta = 1/32\omega_0$, $W_0^{(0)} = -1/2$, $k_{1,2} = 0$, $\nu_1 = 0.7\omega_0$, $\nu_2 = 0.4\omega_0$, and $X = -120\omega_0$ (a), $X = 0.95\omega_0$ (b), $X = 130\omega_0$ (c).

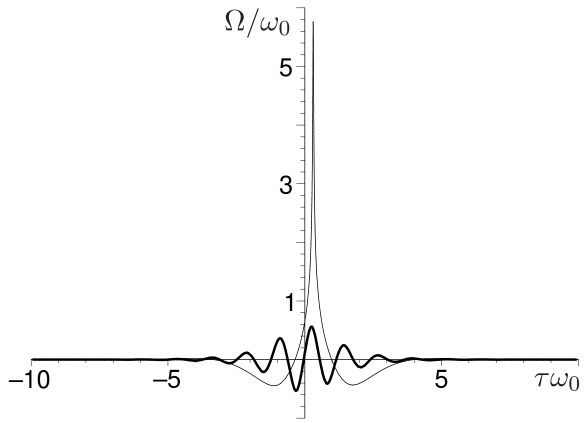

Fig. 4 – Profiles of the variable Ω of breather solution with parameters $\beta = 1/32\omega_0$, $W_0^{(0)} = -1/2$, $X = 0.75\omega_0$, $\nu_R = \omega_0$ and $\nu_I = \omega_0$ (normal line), $\nu_I = 5\omega_0$ (bold line).

from above to a finite limit depending on the parameter ν_R then the oscillation of the sharp form with the amplitude exceeding ones of the nearest oscillations in a few times appears.

3.2. THE CASE $\omega_Z < \omega_S$.

The variable Ω_0 of the one-soliton solution of the MRMB equations (38)–(41) is defined as follows:

$$\Omega_0 = \frac{1}{\sigma}\frac{\partial}{\partial T}\arctan\frac{2\sigma^2\exp\theta}{\sigma^2[1-\exp(2\theta)]+\nu^2\tilde{\varepsilon}^2}, \tag{50}$$

where

$$\tilde{\varepsilon} = -\mathrm{i}\varepsilon = \sqrt{-\frac{\beta}{4\omega_0}}.$$

Here, we have

$$\max|\Omega_0| = \left|\frac{\nu}{\sigma}\right|\sqrt{\sigma^2+\nu^2\tilde{\varepsilon}^2}. \tag{51}$$

Substituting expression (50) into Eqs. (42), we obtain an implicit definition of variable Ω of the one-soliton solution of the system (29)–(31), (35). This gives us the following expression for temporal variable:

$$t = 2T + \frac{\tilde{\varepsilon}}{\sigma}\arctan\frac{\sigma^2[1+\exp(2\theta)]-\nu^2\tilde{\varepsilon}^2}{2\sigma\tilde{\varepsilon}\nu} - \left(2\tilde{\varepsilon}^2 W_0 - \frac{1}{\omega_0\alpha a_\perp}\right)X. \tag{52}$$

It is seen from this relation that the one-soliton solution is steady-state. The plot of the variable Ω of the one-soliton solution is presented in Fig. 5.

It follows from Eq. (51) that the amplitude of $|\Omega|$ tends in the limit $|\nu| \to \infty$ to its maximum value $1/|\tilde{\varepsilon}|$. From Eq. (52), we see that the duration of the one-soliton

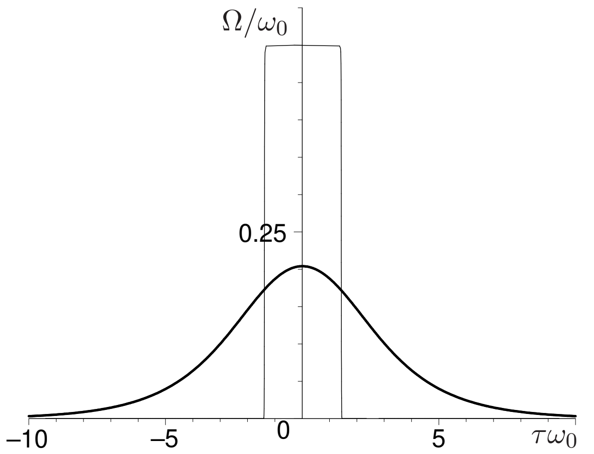

Fig. 5 – Profiles of the variable Ω of one-soliton solution with parameters $\beta = -1/4\omega_0$, $W_0^{(0)} = -1/2$, $X = 0$, and $\nu = 250\omega_0$ (normal line), $\nu = 0.5\omega_0$ (bold line).

solution tends in this limit to the minimal value

$$\tau_{min} = \frac{\pi|\tilde{\varepsilon}|}{|\sigma|}. \tag{53}$$

As a result, the form of the one-soliton solution becomes "rectangular" if $|\nu|$ increases (see Fig. 5).

In the limit $|\nu| \to \infty$, the one-soliton solution of the system (29)–(31), (35) has a compact support. The solutions of such type are known as compactons [21–24, 59].

The expression (53) of minimal duration of the soliton can be written as follows

$$\tau_{min} = \frac{\pi}{\sqrt{\omega_S^2 - \omega_Z^2}}. \tag{54}$$

Since $\omega_S - \omega_Z \ll \omega_S, \omega_Z$, the expression (54) can be rewritten approximately under taking into account (18) in the form

$$\tau_{min} = \frac{\pi}{\sqrt{2\omega_Z\omega_0}}. \tag{55}$$

Substituting $\omega_Z \sim 10^{12}$ s^{-1} and $\omega_0 \sim 10^{11}$ s^{-1}, we obtain $\tau_{min} \sim 10^{-11}$–10^{-12} s. Thus, it is necessary to say about the picosecond acoustics of the solid state in this case.

The expression of variable Ω_0 of the two-soliton solution of the MRMB equations (38)–(41) has the form

$$\Omega_0 = \frac{1}{\sigma}\frac{\partial}{\partial T}\left(\arctan\frac{\sigma(\nu_1+\nu_2)\tilde{s}_+}{\tilde{r}_-} + \arctan\frac{\sigma(\nu_1+\nu_2)\tilde{s}_-}{\tilde{r}_+}\right), \tag{56}$$

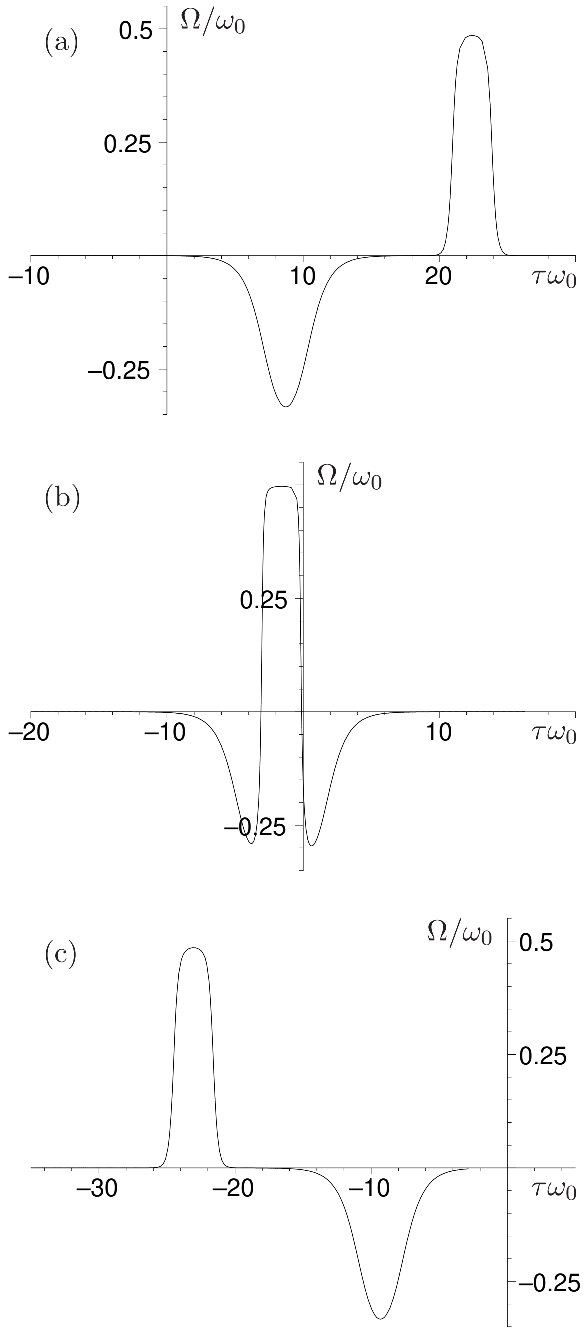

Fig. 6 – Profiles of the variable Ω of two-soliton solution with parameters $\beta = -1/4\omega_0$, $W_0^{(0)} = -1/2$, $k_{1,2} = 0$, $\nu_1 = -\omega_0$, $\nu_2 = -4.5\omega_0$, and $X = -25\omega_0$ (a), $X = 0$ (b), $X = 25\omega_0$ (c).

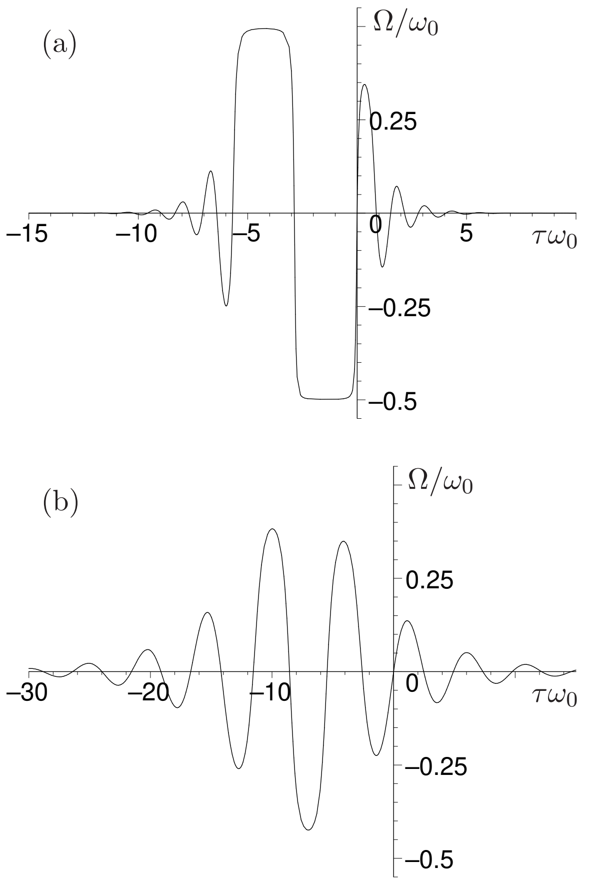

Fig. 7 – Profiles of the variable Ω of breather solution with parameters $\beta = -1/4\omega_0$, $W_0^{(0)} = -1/2$, $X = 0$, and $\nu_R = \omega_0$, $\nu_I = 5\omega_0$ (a), $\nu_R = 0.2\omega_0$, $\nu_I = 1.3\omega_0$ (b).

where

$$\tilde{s}_\pm = \sigma[\exp(-\theta_1) - \exp(-\theta_2)] \pm \tilde{\varepsilon}(\nu_1 - \nu_2)\exp(-\theta_1 - \theta_2),$$

$$\tilde{r}_\pm = (\nu_1 - \nu_2)\left[\sigma^2 + (\sigma^2 - \tilde{\varepsilon}^2\nu_1\nu_2)\exp(-\theta_1 - \theta_2)\right] \\ \pm\sigma\tilde{\varepsilon}(\nu_1 + \nu_2)\left[\nu_1\exp(-\theta_1) - \nu_2\exp(-\theta_2)\right].$$

Substitution of the expression (56) into Eqs. (42) defines implicitly the variable Ω of the two-soliton solution of the system (29)–(31), (35). The plot of variable Ω in the case of the collision of solitons with the opposite polarities is presented in Fig. 6.

The variable Ω_0 of the breather solution of the MRMB equations (38)–(41) is written as follows

$$\Omega_0 = \frac{1}{\sigma}\frac{\partial}{\partial T}\left(\arctan\frac{\nu_R q_-}{\nu_I p_-} - \arctan\frac{\nu_R q_+}{\nu_I p_+}\right), \tag{57}$$

where

$$p_{\pm} = \sigma + \tilde{\varepsilon}\nu_I \pm 2\tilde{\varepsilon}\nu_R \sin(\theta_I)\exp(-\theta_R) + (\sigma - \tilde{\varepsilon}\nu_I)\exp(-2\theta_R),$$

$$q_{\pm} = p_{\pm} - \sigma[1 \mp 2\cos(\theta_I)\exp(-\theta_R) + \exp(-2\theta_R)].$$

The implicit definition of the variable Ω of the breather solution of the system (29)–(31), (35) is obtained by substituting the expression (57) into Eqs. (42). The profiles of the variable Ω of this solution are presented in Fig. 7.

If $|\nu_I| > |\sigma/\tilde{\varepsilon}|$ and $\nu_R \to 0$, then the form of two oscillations in the center of breather becomes "rectangular" (see Fig. 7a). The amplitude and duration of the "rectangular" oscillations are close to $1/|\tilde{\varepsilon}|$ and τ_{min}, respectively.

Thus, the oscillations of the breather have the rectangular form in the case $\omega_I > \omega_0$. If $\omega_I < \omega_0$, then the breather oscillations gradually take the sinusoidal form with further reduction of the central frequency ω_I of the spectrum of the acoustic signal (Fig. 7b).

4. CONCLUSION

In this paper, the solitonic modes of the propagation of pulses of the strain deformation in a crystal containing paramagnetic impurities possessing the effective spin $S = 1$ are investigated. The crystal is placed into an external magnetic field $\mathbf{B}$ and is subjected to the longitudinal static deformation in the direction of $\mathbf{B}$. The magnetic field causes equidistant Zeeman splitting ω_Z of the spin sublevels on three states. In turn, the static deformation creates gradients of the electric field in the crystal owing to the van Vleck mechanism. As a result, there is the Stark shift ω_S of the middle spin sublevel with respect to the lower and upper Zeeman sublevels.

Considering effectively the third quantum level, we have reduced the material equations for spin dynamics to the case of a two-level system. Having applied the approximation of the unidirectional propagation to the wave equation, we obtained the self-consistent nonlinear system (29)–(31), (35). From the formal point of view, this system represents a generalization of the system of reduced Maxwell–Bloch equations and is integrable by the inverse scattering transformation method.

It is revealed that the dynamics of the solitons described by the system we have studied in this work is very sensitive to the ratio between frequencies ω_Z and ω_S. If $\omega_Z > \omega_S$, then the solitons and breathers of relative deformation with the pointed profiles are formed. The interaction of such solitons with opposite polarities can lead to the appearance of a large-amplitude short-living pulse having the dynamics similar to that of rogue waves. In the case $\omega_Z < \omega_S$, the profiles of solitons and breathers, on the contrary, are blunted. Also, there is the minimal duration τ_{min} of the soliton (see. (53)) that corresponds to the rectangular profile.

For the velocity of the transverse elastic wave in a crystal MgO, we have $a \approx 3 \cdot 10^5$ cm/s [41]. Taking the minimal duration $\tau_{min} \sim 10^{12}$ s, we find that the spatial size of such soliton is $l \sim 10^{-6}$–10^{-7} cm, which is comparable on the order of magnitude with the period of a crystal lattice. In this case, the approximation of the continuous medium is inapplicable, and it is necessary to consider the spatial dispersion caused by the discrete structure of the crystal [60]. We are planning to take this effect into account in our future researches.

Acknowledgements. This work was supported by the Russian Science Foundation (Project No 17–11–01157).

REFERENCES

1. S. L. McCall and E. L. Hahn, Phys. Rev. Lett. **18**, 908 (1967).
2. S. L. McCall and E. L. Hann, Phys. Rev. **183**, 457 (1969).
3. G. L. Lamb, Jr, Rev. Mod. Phys. **43**, 99 (1971).
4. I. A. Poluektov, Y. M. Popov, and V. S. Roitberg, Sov. Phys.-Usp. **18**, 673 (1975).
5. L. Allen and J. H. Eberly, *Optical Resonance and Two-Level Atoms*, John Wiley & Sons, NY, 1975.
6. G. L. Lamb, Jr, *Elements of Soliton Theory*, John Wiley & Sons, NY, 1980.
7. R. K. Dodd, J. C. Eilbeck, J. Gibbon, and H. C. Morris, *Solitons and Nonlinear Wave Equations*, Academic Press, NY, 1982.
8. A. I. Maimistov, A. M. Basharov, S. O. Elyutin, and Y. M. Sklyarov, Phys. Rep. C **191**, 1 (1990).
9. M. J. Ablowitz and P. A. Clarkson, *Solitons, Nonlinear Evolution Equations and Inverse Scattering*, Cambridge University Press, Cambridge, 1991.
10. A. R. Osborne, *Nonlinear Ocean Waves and the Inverse Scattering Transform*, Academic Press, NY, 2010.
11. J. C. Eilbeck, J. D. Gibbon, P. J. Caudrey, and R. K. Bullough, J. Phys. A **6**, 1337 (1973).
12. E. M. Belenov and A. V. Nazarkin, JETP Lett. **51**, 288 (1990).
13. E. M. Belenov, A. V. Nazarkin, and V. A. Ushchapovskii, Sov. Phys. JETP **73**, 422 (1991).
14. S. A. Kozlov and S. V. Sazonov, JETP **84**, 221 (1997).
15. I. V. Melnikov, D. Mihalache, F. Moldoveanu, and N.-C. Panoiu, Phys. Rev. A **56**, 1569 (1997).
16. S. V. Sazonov, JETP **92**, 361 (2001).
17. H. Leblond, S. V. Sazonov, I. V. Melnikov, D. Mihalache, and F. Sanchez, Phys. Rev. A **74**, 063815 (2006).
18. H. Leblond and D. Mihalache, Phys. Rep. **523**, 61 (2013).
19. D. Mihalache, Rom. Rep. Phys. **69**, 403 (2017).
20. S. V. Sazonov, Rom. Rep. Phys. **70**, 401 (2018).
21. S. V. Sazonov, JETP **119**, 423 (2014).
22. S. V. Sazonov and N. V. Ustinov, Phys. Rev. A **98**, 063803 (2018).
23. S. V. Sazonov and N. V. Ustinov, Phys. Rev. A **100**, 053807 (2019).
24. N. V. Ustinov, J. Math. Phys. **60**, 013503 (2019).
25. F. V. Bunkin, Y. A. Kravtsov, and G. A. Lyakhov, Sov. Phys.-Usp. **29**, 607 (1986).
26. S. A. Akhmanov and V. E. Gusev, Sov. Phys.-Usp. **35**, 153 (1992).
27. N. S. Shiren, Phys. Rev. B **2**, 2471 (1970).

28. J. R. Fletcher, J. Phys. C **3**, 1349 (1970).
29. G. A. Denisenko, Sov. Phys. JETP **33**, 1220 (1971).
30. V. V. Samartsev, B. P. Smolyakov, and R. Z. Sharipov, JETP Lett. **20**, 296 (1974).
31. G. T. Adamashvili, Physica B **266**, 173 (1999).
32. A. A. Zabolotskii, JETP **96**, 1089 (2003).
33. A. A. Zabolotskii, Physica D **185**, 117 (2003).
34. A. A. Zabolotskii, Phys. Rev. E **67**, 066606 (2003).
35. A. V. Gulakov and S. V. Sazonov, J. Phys. Condens. Matter **16**, 1733 (2004).
36. S. V. Sazonov and N. V. Ustinov, Phys. Rev. E **73**, 056614 (2006).
37. A. A. Zabolotskii, JETP **105**, 439 (2007).
38. S. V. Sazonov and N. V. Ustinov, J. Phys. A: Math. Theor. **40**, F551 (2007).
39. S. V. Sazonov and N. V. Ustinov, Phys. Solid State **50**, 1122 (2008).
40. S. V. Sazonov and N. V. Ustinov, JETP **114**, 645 (2012).
41. J. W. Tucker and V. W. Rampton, *Microwave Ultrasonics in Solid State Physics*, North-Holland Publishing Company, Amsterdam, 1972.
42. E. H. Jacobsen and K. W. H. Stevens, Phys. Rev. **129**, 2036 (1963).
43. V. B. Matveev and M. A. Salle, *Darboux Transformations and Solitons*, Springer-Verlag, Berlin-Heidelberg, 1991.
44. V. G. Bagrov and B. F. Samsonov, Theor. Math. Phys. **104**, 1051 (1995).
45. C. Gu, A. Hu, and Z. Zhou, *Darboux Transformations in Integrable Systems*, Springer Science and Business Media, Dordrecht, 2005.
46. A. V. Slyunyaev, JETP **92**, 529 (2001).
47. E. G. Shurgalina and E. N. Pelinovsky, Phys. Lett. A **380**, 2049 (2016).
48. C. Kharif, E. Pelinovsky, and A. Slunyaev, *Rogue Waves in the Ocean*, Springer, Berlin, 2009.
49. M. Onorato, S. Residori, U. Bortolozzo, A. Montina A, and F. T. Arecchi, Phys. Rep. **528**, 47 (2013).
50. J. M. Dudley, F. Dias, M. Erkintalo, and G. Genty, Nat. Photonics **8**, 755 (2014).
51. N. Akhmediev *et al.*, J. Opt. **18**, 063001 (2016).
52. S. Chen, F. Baronio, J. M. Soto-Crespo, P. Grelu, and D. Mihalache, J. Phys. A: Math. Theor. **50**, 463001 (2017).
53. E. G. Charalampidis, J. Cuevas-Maraver, D. J. Frantzeskakis, and P. G. Kevrekidis, Rom. Rep. Phys. **70**, 504 (2018).
54. B. A. Malomed and D. Mihalache, Rom. J. Phys. **64**, 106 (2019).
55. J. M. Dudley, G. Genty, A. Mussot, A. Chabchoub, and F. Dias, Nat. Rev. Phys. **1**, 675 (2019).
56. C. B. Ward and P. G. Kevrekidis, Rom. J. Phys. **64**, 112 (2019).
57. Y. Song, Z. Wang, C. Wang, K. Panajotov, and H. Zhang, Advanced Photonics **2**, 024001 (2020).
58. C. Hou, L. Bu, F. Baronio, D. Mihalache, and S. Chen, Rom. Rep. Phys. **72**, 405 (2020).
59. P. Rosenau and A. Zilburg, J. Phys. A: Math. Theor. **51**, 343001 (2018).
60. S. V. Sazonov, J. Phys. Condens. Matter **6**, 6295 (2004).